International Journal of Technical Innovation in Modern Engineering & Science (IJTIMES)
Impact Factor: 5.22 (SJIF-2017), e-ISSN: 2455-2585
Volume 5, Issue 09, September-2019

Numerical Study of Non-Darcy Mixed Convective Heat and Mass Transfer Flow in a Cylindrical Annulus with Chemical Reaction and Heat Sources

Palla Kristaiah

Assistant Professor in Mathematics, Dr.A.P.J.Abdul Kalam, I.I.I.T., R.G.U.K.T., Ongole, A.P., India

Abstract : ***We analyse the non-Darcy free and forced convection flow through a porous medium in a Co-axial cylindrical duct where the boundaries are maintained at temperature Tw and Concentration Cw. The behaviour of velocity, temperature and concentration is analyzed at different axial positions. The shear stress and the rate of heat and mass transfer have also been obtained for variations in the governing parameters.***

Keywords: Heat and Mass transfer, Cylindrical Annulus, Chemical Reaction, Heat Sources

1. INTRODUCTION:

Transport phenomena involving the combined influence of thermal and concentration buoyancy are often encountered in many engineering systems and natural environments. There are many applications of such transport processes in the industry, notably in chemical distilleries, heat exchangers, solar energy collectors and thermal protection systems. In all such classes of flows, the driving force is provided by a combination of thermal and chemical diffusion effects. In atmosphere flows, thermal convection of the earth by sunlight is affected by differences in water vapour concentration. This buoyancy driven convection due to coupled heat and mass transfer in porous media has also many important applications in energy related engineering. These include moisture migration, fibrous insulation, spreading of chemical pollution in saturated soils, extraction of geothermal energy and underground disposal of natural waste.

Chen and Yuh (4) have investigated the heat and mass transfer characteristics of natural convection flow along a vertical cylinder under the combined buoyancy effects of thermal and species diffusion, Sivanjaneya Prasad (11) has investigated the free convection flow of an incompressible, viscous fluid through a porous medium in the annulus between the porous concentric cylinders under the influence of a radial magnetic field. Antonio (2) has investigated the laminar flow, heat transfer in a vertical cylinder duct by taking into account both viscous dissipation and the effect of buoyancy, the limiting case of fully developed natural convection in porous annuli is solved analytically for steady and transient cases by E. Sharawi and Al-Nimir (10) and Al-Nimir (1). Philip (8) has obtained solutions for the annular porous media valid for low modified Reynolds number. Chamkha et al. (3) studied the effect of radiation on combined heat and mass transfer by non-Darcy natural convection about an impermeable horizontal cylinder embedded in porous medium.

The effect of radial magnetic fields on convective heat and mass transfer flow in cylindrical annulus has been investigated by several authors under varied conditions (Sreevani (13), Prasad (9), Reddy (12), Sudheer Kumar *et. al.*, (15), Padmavathi (7), Madhusudhan Reddy (5), Sudarsana Reddy et al(14), Mallikarjuna et al(6)).

In this paper we discuss the non-Darcy free and forced convection flow through a porous medium in a Co-axial cylindrical duct where the boundaries are maintained at temperature Tw and Concentration Cw. The behaviour of velocity, temperature and concentration is analyzed at different axial positions. The shear stress and the rate of heat and mass transfer have also been obtained for variations in the governing parameters.

2. FORMULATION OF THE PROBLEM:

We consider the free and forced convection flow in a vertical circular annulus through a porous medium whose walls are maintained at a constant heat flux and uniform concentration. The flow, temperature and concentration in the fluid are assumed to be fully developed. Both the fluid and porous region have constant physical properties and the flow is a mixed convection flow taking place under thermal and molecular buoyancies and uniform axial pressure gradient. The Boussinesque approximation is invoked so that the density variation is confined to the thermal and molecular buoyancy forces. The Brinkman-Forchhimer-Extended Darcy model which accounts for the inertia and boundary effects has been used for the momentum equation in the porous region. The momentum, energy and diffusion equations are coupled and non-linear. Also the flow is unidirectional along the axial direction of the cylindrical annulus. Making use of the above assumptions the governing equations are

$$-\frac{\partial p}{\partial z}+\frac{\nu}{\delta}\left(\frac{\partial^2 u}{\partial r^2}+\frac{1}{r}\frac{\partial u}{\partial r}\right)-(\frac{\nu}{k})u-\frac{\sigma u_e^2 H_0^2}{r^2}-\frac{\delta F}{\sqrt{k}}u^2+\rho\beta(T-T_i)+\rho\beta^{\bullet}(C-C_i)=0 \qquad (1)$$

$$\rho C_p u \frac{\partial T}{\partial z} = k_f \left(\frac{\partial^2 T}{\partial r^2} + \frac{1}{r} \frac{\partial T}{\partial r} \right) + Q_H (T - T_0) - \frac{\partial (q_R)}{\partial y} \quad (2)$$

$$u \frac{\partial C}{\partial z} = D_B \left(\frac{\partial^2 C}{\partial r^2} + \frac{1}{r} \frac{\partial C}{\partial r} \right) - k_c^{'} C \quad (3)$$

where u is the axial velocity in the porous region, T , C are the temperature and concentration of the fluid, k is the permeability of porous medium, k_f is the thermal diffusivity, F is a function that depends on Reynolds number, the microstructure of the porous medium and D_B is the molecular diffusivity, β is the coefficient of the thermal expansion, Q_H is the heat source coefficient, $Q_1^{'}$ is the radiation absorption coefficient,C p is the specific heat, ρ is density and g is gravity .

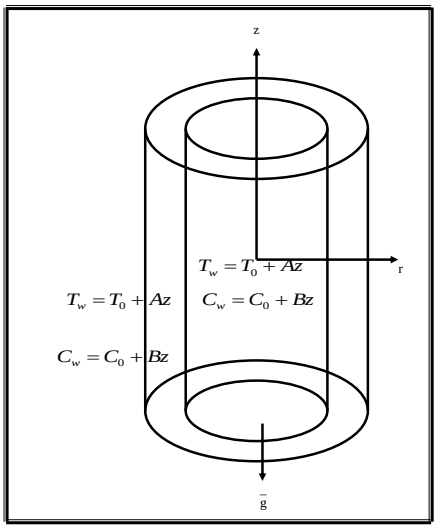

Fig.1 : CONFIGURATION OF THE PROBLEM

The relevant boundary conditions are

$u = 0$, $T=T_w$, $C=C_w$ at r = a&a+s (4)

Following Tao(28a),we assume that the temperature and concentration of the both walls is $T_w = T_0 + Az$, $C_w = C_0 + Bz$ where A and B are the vertical temperature and concentration gradients which are positive for buoyancy –aided flow and negative for buoyancy –opposed flow,respectively, T_0 and C_0 are the upstream reference wall temperature and concentration ,respectively.For the fully developed laminar flow in the presences of radial magnetic field,the velocity depend only on the radial coordinate and all the other physical variables except temperature,concentration and pressure are functions of r and z, z being the vertical co-ordinate .The temperature and concentration inside the fluid can be written as

$$T = T^{\bullet}(r) + Az \quad , \quad C = C^{\bullet}(r) + Bz \quad (5)$$

By applying Rosseland approximation (Brewester) the radiative heat flux q_r is given by

$$q_r = -\left(\frac{4\sigma^*}{3\beta_R} \right) \frac{\partial}{\partial y} \left[T'^4 \right] \quad (6)$$

where σ* is the Stephan – Boltzmann constant

β_R is the mean absorption coefficient.

Expanding T'^4 about T_e in Taylor Series we get

$$T'^4 = 4T_e^3 T - 3T_e^4 .$$

The energy equations reduces to

$$\rho C_p u \frac{\partial T}{\partial z} = k_f \left(\frac{\partial^2 T}{\partial r^2} + \frac{1}{r} \frac{\partial T}{\partial r} \right) + Q_H (T - T_0) + \frac{16\sigma^{\bullet} T_e^3}{3\beta_R} \left(\frac{\partial^2 T}{\partial r^2} + \frac{1}{r} \frac{\partial T}{\partial r} \right) \quad (7)$$

We now define the following non-dimensional variables

$$z^* = \frac{z}{a} \quad , \quad r^* = \frac{r}{a} \quad , \quad u^* = (\frac{a}{\nu})u$$

$$p^* = \frac{pa\delta}{\rho \nu^2} \quad , \quad \theta^*(r^{\bullet}) = \frac{T^{\bullet} - T_0}{Aa} \quad , \quad C^*(r^{\bullet}) = \frac{C^{\bullet} - C_0}{Ba} \quad , \quad , \quad s^* = \frac{s}{a}$$

Introducing these non-dimensional variables,the governing equations in the non-dimensional form are (on removing the stars)

$$(\frac{\partial^2 u}{\partial r^2}+\frac{1}{r}\frac{\partial u}{\partial r}) = 1+\delta(D^{-1}+\frac{M^2}{r^2})u+\delta^2(D^{-1})^{1/2}\Lambda u^2-\delta G(\theta+NC)$$

$$(1+\frac{4Rd}{3})(\frac{\partial^2\theta}{\partial r^2}+\frac{1}{r}\frac{\partial\theta}{\partial r}) = u+\frac{\alpha}{\Pr}\theta$$

$$(\frac{\partial^2 C}{\partial r^2}+\frac{1}{r}\frac{\partial C}{\partial r})-\gamma C = Sc\,u \qquad (8)$$

where

$\Lambda = FD^{-1}$ (Inertia parameter or Forchhimer number), $G=\frac{g\beta(T_e-T_i)a^3}{\nu^2}$ (Grashof number), $D^{-1}=\frac{a^2}{k}$ (Inverse Darcy parameter), $M^2=\frac{\sigma\mu_e^2H_0^2}{a\nu}$ (Hartmann number), $P_r=\frac{\mu C_p}{k_f}$ (Prandtl number) $Sc=\frac{\nu}{D_B}$ (Schmidt number), $\gamma=\frac{k_c^1a^2}{DB}$ (Chemical Reaction parameter), $Rd=\frac{4\sigma^{\bullet}T_e^3}{\beta_R k_f}$ (Radiation parameter)

The corresponding non-dimensional conditions are

$u=0$, $\theta=0$, C=0 at r=1 and 1+s (9)

3. FINITE ELEMENT ANALYSIS

The finite element analysis with quadratic polynomial approximation functions is carried out along the radial distance across the circular duct. The behavior of the velocity, temperature and concentration profiles has been discussed computationally for different variations in governing parameters. The Gelarkin method has been adopted in the variational formulation in each element to obtain the global coupled matrices for the velocity, temperature and concentration in course of the finite element analysis.

Choose an arbitrary element e_k and let u^k, θ^k and C^kbe the values of u, θ and C in the element e_k

We define the error residuals as

$$E_p^k=\frac{d}{dr}\left(r\frac{du^k}{dr}\right)+\delta G(\theta^k)-\delta(D^{-1}+\frac{M^2}{r^2})ru^k-\delta^2\Lambda r(u^k)^2 \qquad (10)$$

$$E^k{}_\theta=\frac{1}{\Pr}\frac{d}{dr}\left(r\frac{d\theta^k}{dr}\right)-ru^k+\frac{\alpha}{P_r}r\theta \qquad (11)$$

$$E^k{}_c=\frac{d}{dr}\left(r\frac{dC^k}{dr}\right)-rScu^k-\gamma C^k \qquad (12)$$

where u^k, θ^k & C^k are values of u, θ& C in the arbitrary element e_k. These are expressed as linear combinations in terms of respective local nodal values.

$$u^k=u_1^k\psi_1^k+u_2^k\psi_1^k+u_3^k\psi_3^k$$

$$\theta^k=\theta_1^k\psi_1^k+\theta_2^k\psi_2^k+\theta_3^k\psi_3^k$$

$$C^k=C_1^k\psi_1^k+C_2^k\psi_2^k+C_3^k\psi_3^k$$

where ψ_1^k, ψ_2^k --------- etc are Lagrange's quadratic polynomials.

Following the Gelarkin weighted residual method and integrating by parts equations (10) - (12) we obtain

$$\int_{rA_1}^{rB_1} r\frac{du^k}{dr}\frac{d\psi_j^k}{dr}dr-\delta G\int_{rA_1}^{rB_1} r(\theta^k)\psi_j^k dr+\delta(M_1{}^2)\int_{rA_1}^{rB_1} ru^k\psi_j^k dr+\delta^2\Lambda\int_{rA_1}^{rB_1} r(u^k)^2\psi_j^k dr=Q_{2\,j}^k+Q_{1\,j}^k-P\int_{rA_1}^{rB_1} r\psi_j^k dr \qquad (13)$$

$$-Q_{1\,j}^k=\left[\left(\frac{du^k}{dr}\right)(r\psi_j^k)\right]r_{A_1} \quad , \quad -Q_{2\,j}^k=\left[\left(\frac{du^k}{dr}\right)(r\psi_j^k)\right]r_{B_1}$$

$$\int_{rA_1}^{rB_1} r\frac{d\theta^k}{dr}\frac{d\psi_j{}^k}{dr}dr+\alpha\int_{rA_1}^{rB_1} r\theta^k dr-P_r\int_{rA_1}^{rB_1} ru^k\psi_j^k dr+R_{2\,j}^k+R_{1\,j}^k \qquad (14)$$

$$-R_{1\,j}^k=\left[\left(\frac{d\theta^k}{dr}\right)(r\psi_j^k)\right]r_{A_1} \quad , \quad R_{2\,j}^k=\left[\left(\frac{d\theta^k}{dr}\right)(r\psi_j^k)\right]r_{B_1}$$

$$\int_{rA_1}^{rB_1} r\frac{dC^k}{dr}\frac{d\psi_j{}^k}{dr}dr-\gamma\int_{rA_1}^{rB_1} rC^k dr=Sc\int_{rA_1}^{rB_1} ru^k\psi_j^k dr+S_{2\,j}^k+S_{1\,j}^k \tag{15}$$

$$-S_{1\,j}^k=\left[\left(\frac{dC^k}{dr}\right)(r\psi_j^k)\right]r_{A_1}\quad,\qquad S_{2\,j}^k=\left[\left(\frac{dC^k}{dr}\right)(r\psi_j^k)\right]r_{B_1}$$

Expressing u^k, θ^k, C^k in terms of local nodal values in (13) - (15) we obtain

$$\sum_{i=1}^{3}u^k\int_{rA_1}^{rB_1} r\frac{d\psi_i^k}{dr}\frac{d\psi_j^k}{dr}dr-\delta G\sum_{i=1}^{3}(\theta_i^k)\int_{rA_1}^{rB_1} r\psi_i^k\psi_j^k dr+\frac{1}{A_1A_3}\delta(D^{-1}\sum_{i=1}^{3}\int_{rA_1}^{rB_1} r\psi_i^k\psi_j^k dr$$
$$+M^2\sum_{i=1}^{3}\int_{rA_1}^{rB_1}(1/r)\psi_i^k\psi_j^k dr)+\delta^2\Lambda\sum_{i=1}^{3}u_i^k\int_{rA_1}^{rB_1} rU_i^k\psi_i^k\psi_j^k dr=Q_{2\,j}^j+Q_{1\,j}^k \tag{16}$$
$$-P\int_{rA_1}^{rB_1} r\psi_i^k\psi_j^k dr$$

$$\frac{1}{\Pr}\sum_{i=1}^{3}\theta_i^k\int_{rA_1}^{rB_1} r\frac{d\psi_i^k}{dr}\frac{d\psi_j^k}{dr}dr-\sum_{i=1}^{3}u_i^k\int_{rA_1}^{rB_1} r\psi_i^k\psi_j^k dr+$$
$$+\alpha\sum_{i=1}^{3}\theta_i^k\int_{rA_1}^{rB_1} r\psi_i^k\psi_j^k dr=R_{2\,j}^k+R_{1\,j}^k \tag{17}$$

$$\sum_{i=1}^{3}C_i^k\int_{rA_1}^{rB_1} r\frac{d\psi_i^k}{dr}\frac{d\psi_j^k}{dr}dr-\gamma\sum_{i=1}^{3}C_i^k\int_{rA_1}^{rB_1} r\psi_i^k\psi_j^k dr+Sc\sum_{i=1}^{3}u_i^k\int_{rA_1}^{rB_1} r\psi_i^k\psi_j^k dr+ \tag{18}$$
$$r=S_{2\,j}^k+S_{1\,j}^k$$

Choosing different ψ_j^k's corresponding to each element e_k in the equation (16) yields a local stiffness matrix of order 3×3 in the form

$$(f_i^k{}_j)(u_i^k)-(\frac{A_4}{A_2A_3})\delta G(g_i^k{}_j)(\theta_i^k)+\delta D^{-1}(m_i^k{}_j)(u_i^k)+$$
$$\delta M^2(m_i^k{}_j)(u_i^k)+\delta^2\Lambda(n_i^k{}_j)(u_i^k)=(Q_{2\,j}^k)+(Q_{1\,j}^k)+(v_j^k) \tag{19}$$

Likewise the equation (17) & (18) give rise to stiffness matrices

$$(1+\frac{4Rd}{3})(e_i^k{}_j)(\theta_i^k)+\alpha(f_i^k{}_j)(\theta_i^k)-(t_i^k{}_j)(u_i^k)=R_{2\,j}^k+R_{1\,j}^k \tag{20}$$

$$(l_i^k{}_j-k)(C_i^k)-(t_i^k{}_j)(u_i^k)=S_{2\,j}^k+S_{1\,j}^k \tag{21}$$

where $(f_i^k{}_j)$, $(g_i^k{}_j)$, $(m_i^k{}_j)$, $(n_i^k{}_j)$, $(e_i^k{}_j)$, $(l_i^k{}_j)$ and $(t_i^k{}_j)$ are 3×3 matrices and $v_j^k=-P_1\int_{rA_1}^{rB_1} r\psi_i^k\psi_j^k dr$ and $(Q_{2\,j}^k)$, $(Q_{1\,j}^k)$, $(R_{2\,j}^k)$ & $(R_{1\,j}^k)$, $(S_{2\,j}^k)$ & $(S_{1\,j}^k)$ are 3×1 column matrices. Such stiffness matrices (18) - (20) in terms of local nodes in each element are assembled using interelement continuity and equilibrium conditions to obtain the coupled global matrices in terms of the global nodal values of u, θ & C in the region.

The ultimate coupled global matrices are solved to determine the unknown global nodal values of the velocity, temperature and concentration in fluid region. In solving these global matrices an iteration procedure has been adopted to include the boundary and effects in the porous medium. This procedure is repeated till the consecutive values of u_i's, θ_i's and C_i's differ by a preassigned percentage.

4. SHEAR STRESS, NUSSELT NUMBER AND SHERWOOD NUMBER

The shear stress (τ) is evaluated using the formula $\tau=(\frac{du}{dr})_{r=1,1+s}$

The rate of heat transfer (Nusselt number) is evaluated using the formula $Nu=-(\frac{d\theta}{dr})_{r=1,1+s}$

The rate of mass transfer (Sherwood number) is evaluated using the formula $Sh = -(\frac{dC}{dr})_{r=1,1+s}$

5. COMPARISON: In the absence of thermo-diffusion(So=0) the results are in good agreement with **Madhusudan Reddy et al (5).**

Parameters			**Madhusudana Reddy et al(5)**				**Present results(So=0)**			
N	Rd	γ	Nu(1)	Nu(2)	Sh(1)	Sh(2)	Nu(1)	Nu(2)	Sh(1)	Sh(2)
1	0.5	0.5	0.10673	1.7335	12.3727	14.5232	0.10669	1.7336	12.36987	14.52289
2	0.5	0.5	0.11549	1.74131	12.3734	14.5233	0.11538	1.741299	12.37299	14.52319
-0.5	0.5	0.5	0.01152	1.74152	12.3718	14.5237	0.011492	1.741499	12.3714	14.52299
-1.5	0.5	0.5	0.01156	1.74162	12.3712	14.5138	0.01151	1.74155	12.3706	14.5136
1	1.5	0.5	0.2225	3.3518	12.3721	14.5237	0.22239	3.35168	12.3719	14.5231
1	5.0	0.5	0.30165	4.5736	12.3713	14.5239	0.30159	4.57345	12.3709	14.52301
1	0.5	1.5	0.11552	1.74131	13.0332	14.4276	0.115499	1.74131	13.03289	14.4266
1	0.5	-0.5	0.11554	1.741525	13.3226	14.4516	0.115035	1.741499	13.32189	14.4516
1	0.5	-1.5	0.11543	1.741625	12.1728	14.4526	0.115437	1.741587	12.17187	14.4522

6. RESULTS AND DISCUSSION

In order to get physical Insight into the problem we have carried out numerical calculations for non-dimensional velocity, temperature and spices concentration, skin-friction, Nusselt number and Sherwood number by assigning some specific values to the parameters entering into the problem

Effects of parameters on velocity profiles:

Fig.2 exhibits the variation of u with buoyancy ratio(N).It is found that when the molecular buoyancy force dominates over the thermal buoyancy force the axial velocity reduces when the buoyancy forces are in the same direction and for the forces acting in opposite directions it enhances in magnitude.

The effect of chemical reaction parameter(γ) on u is exhibited in fig.3.It is found that the axial velocity enhances with increase in γ>0, in the degenerating chemical reaction case and in the generating chemical reaction case ,the velocity reduces in magnitude in the entire flow region.

Fig.4 shows the variation of u with heat source parameter (α).It is found that an increase in the strength of the heat generating / source(|α|>0) larger the velocity in the entire flow region and in the case of heat absorbing source ,we notice a decrease in the velocity in the flow region..

Fig.5 represent the variation of u with Forchhimer parameter (Λ) .An increase in Λ reduces the velocity in the entire channel This is due to the fact that increasing Λ reduces the momentum boundary layer in the floe region of the channel.

Fig.6 shows the variation of u with Rd. It can be seen from the profiles that the axial velocity reduces with increase in Rd. Higher the Radiative heat flux larger the axial velocity. This is due to the fact that increase in Rd reduces the thickness of the momentum boundary layer.

Effects of parameters on temperature profiles:

The non-dimensional temperature(θ) is shown in figs.7-11 for different parametric representation. We follow the convention that the non-dimensional temperature(θ) is positive/negative according as the actual temperature ($T^{\bullet}$) is greater/lesser than the reference temperature(T_o) .

Fig.7 shows the variation of θ with buoyancy ratio(N).It is observed from the profiles that when the molecular buoyancy force dominates over the thermal buoyancy force the actual temperature reduces when the buoyancy forces are in the same direction and for the forces acting in opposite directions the actual temperature increases in the entire flow region.

Fig.8 represents θ with chemical reaction parameter (γ).From the profiles we find that the actual temperature increases with increase in γ in the degenerating chemical reaction case and reduces in the generating chemical reaction case.

Fig.9 exhibits the variation of θ with heat source parameter(α).It is observed from the profiles that an increase in the strength of the heat generating/absorbing source leads to an enhancement in the actual temperature in the flow region. The values of the actual temperature in the case of heat generation source is lesser than that of heat absorbing source. The maximum of θ occurs at r=1.5.

Fig.10 shows the variation of θ with Forchhimer parameter (Λ). As the Λ increases there is a significant increase in the thermal boundary layer with a rise in the actual temperature throughout the flow region, since enhancement of Λ amounts to reduction of thermal diffusion.

Fig.11 shows the variation of temperature (θ) with radiation parameter (Rd). It can be seen from the profiles that the temperature enhances with increase in Rd. This is due to the fact that increase in Rd increases the thickness of the thermal boundary layer.

Effects of parameters on concentration profiles:

The non-dimensional concentration (C) is shown in figs.12-16 for different parametric variations. We follow the convention That the non-dimensional concentration(C) is positive/negative according as the actual concentration ($C^{\bullet}$) is greater/lesser than the reference concentration(C_o) .

Fig.12 shows the variation of C with buoyancy ratio N. We find that when the molecular buoyancy force dominates over the thermal buoyancy force the actual concentration increases in the flow region when the buoyancy forces are in the same direction and for the forces acting in opposite directions the actual concentration reduces in the flow region.

Fig.13 shows the variation of C with Chemical reaction parameter (γ).it can been from the profiles that the actual concentration enhances in the degenerating chemical reaction case while in the generating chemical reaction case we notice a depreciation in the actual concentration in the entire flow region.

Fig.14 shows the variation of C with heat source parameter (α) .An increase in $\alpha>0$, reduces the actual concentration .In the case of heat absorbing source, the actual concentration enhances with increase in the strength of the heat absorbing heat source($|\alpha|>4$) and for higher $|\alpha|\geq 6$,the actual concentration reduces in the flow region.

Fig15. exhibits the variation of C with Forchhimer parameter (Λ). As the Forchhimer parameter increases there is a marginal increase in the actual concentration. This is due to the fact the enhancement of Prandtl number amounts to reduction of thermal diffusion.

Fig.16 shows the variation of C with Sc & Rd. It can be seen from the profiles that the actual concentration enhances with increase in Sc and reduces with Rd. Thus lesser the molecular diffusivity Radiation larger the actual concentration. This is due to the fact that increase in Schmidt number grows the thickness of the concentration boundary layer also the thickness of the concentration boundary layer decays with increase in Rd.

Effects of parameters on Skin friction, Nusselt number and Sherwood number:

The Skin friction, the rate of heat and mass transfer on the inner and outer cylinder r=1&2 is exhibited in table.1.From the tabular values, the molecular buoyancy force dominates over the thermal buoyancy force the skin friction reduces on both the cylinders when the buoyancy forces are in the same direction and for the forces acting in opposite directions it enhances on the inner cylinder and reduces on the outer cylinder. With reference to the chemical reaction parameter(γ) we find that the skin friction enhances in the degenerating chemical reaction case and reduces in the generating chemical reaction case on both the cylinders. As the Forchhimer parameter (Λ) increases the skin friction reduces on the inner cylinder r=1 and enhances on r=2. The skin friction increases at the both the cylinder with increase in Rd.

The rate of heat transfer (Nusselt number) enhances with increase in Λ. With respect to the chemical reaction parameter (γ) we find that the magnitude of Nu enhances in the degenerating chemical reaction case and reduces in the generating chemical reaction case on both the cylinders. When the molecular buoyancy force dominates over the thermal buoyancy force the rate of heat transfer reduces on r=1&2 when the buoyancy forces are in the same direction and for the forces acting in opposite directions, Nu enhances on both the cylinders. The variation of Nu with Λ shows that lesser the thermal diffusivity larger the rate of heat transfer on both the cylinders. An increase in Radiation parameter (Rd) leads to an enhancement in the rate of heat transfer in inner and outer cylinders.

The rate of mass transfer (Sherwood number) enhances with Λ on both the cylinders. An increase in the strength of the heat generating/absorption source reduces Sh on r=1&2.With respect to the chemical reaction parameter (γ) we find that the rate of mass transfer reduces on r=2 and enhances on r=1 in the degenerating chemical reaction case while in generating chemical reaction cases it enhances on r=2 and reduces on r=1.When the molecular buoyancy force dominates over the thermal buoyancy force the rate of mass transfer enhances on r=1 and reduces on r=2 when the buoyancy forces are in the same direction and for the forces acting in opposite directions it reduces on the inner cylinder and enhances on the outer cylinder. As the Forchhimer parameter (Λ) increases we notice an enhancement in Sh on r=1 and depreciation on r=2. The rate of mass transfer grows with increasing in thermal radiation parameter (Rd) at the both the walls.

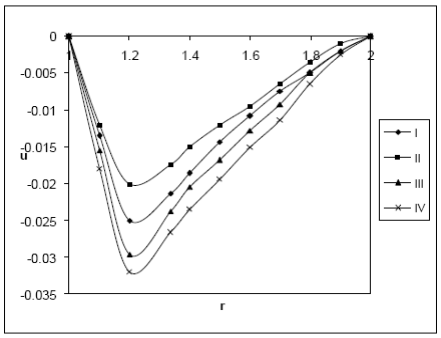

Fig.2 : Variation of u with N

	I	II	III	IV
N	1	2	-0.5	-1.5

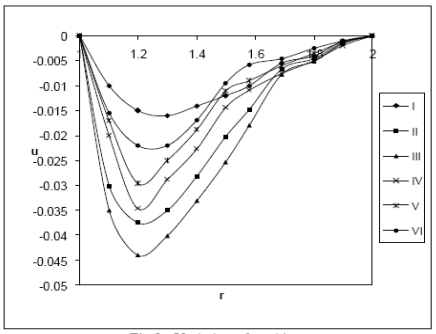

Fig.3 : Variation of u with γ

	I	II	III	IV	V	VI
γ	0.5	1.5	2.5	-0.5	-1.5	-2.5

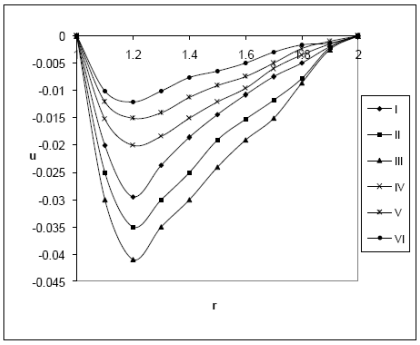

Fig.4 : Variation of u with α

	I	II	III	IV	V	VI
α	2	4	6	-2	-4	-6

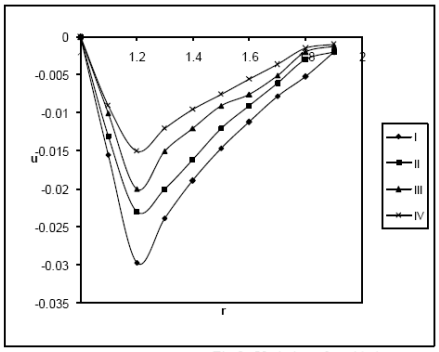

Fig.5 : Variation of u with Λ

	I	II	III	IV
Λ	2	4	6	10

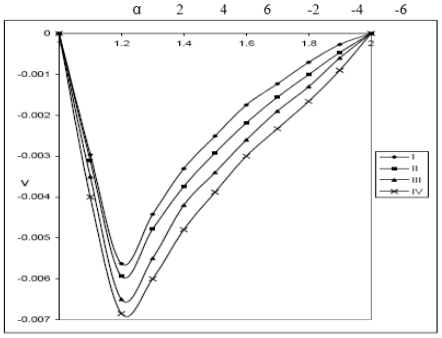

Fig.6 Variation of u with Rd

	I	II	III	IV
Rd	0.5	1.5	3.5	5

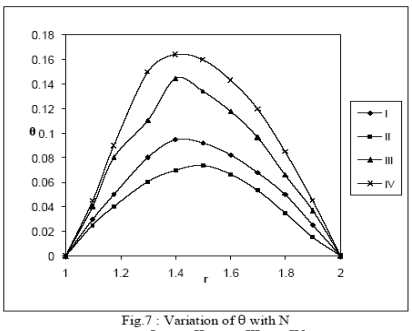

Fig.7 : Variation of θ with N

	I	II	III	IV
N	1	2	-0.5	-1.5

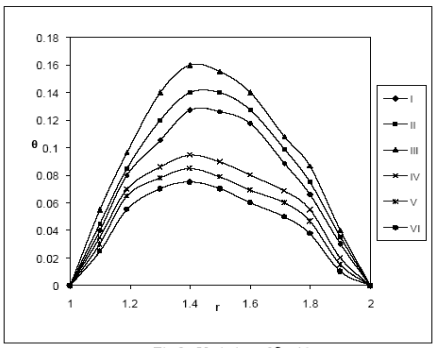

Fig.8 : Variation of θ with γ

	I	II	III	IV	V	VI
γ	0.5	1.5	2.5	-0.5	-1.5	-2.5

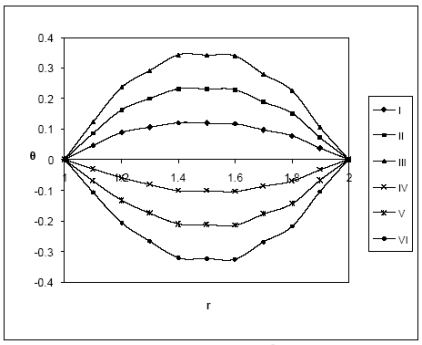

Fig.9 : Variation of θ with α

	I	II	III	IV	V	VI
α	2	4	6	-2	-4	-6

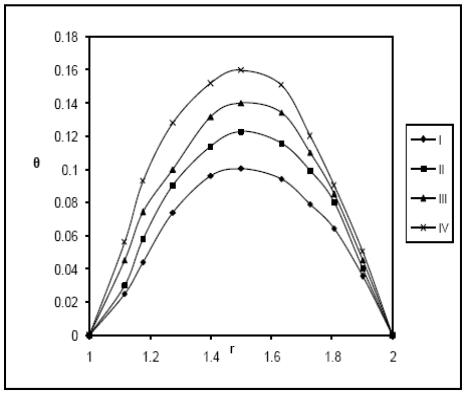

Fig.10 : Variation of θ with Λ

	I	II	III	IV
Λ	2	4	6	10

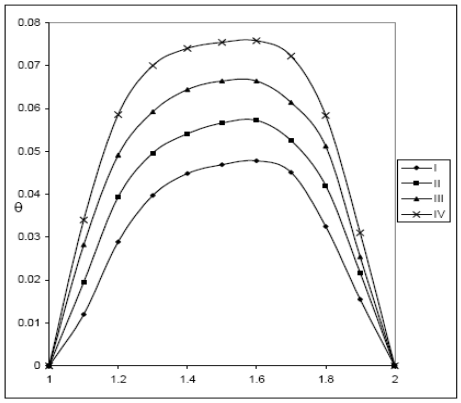

Fig.11 Variation of θ with Rd

	I	II	III	IV
Rd	0.5	1.5	3.5	5

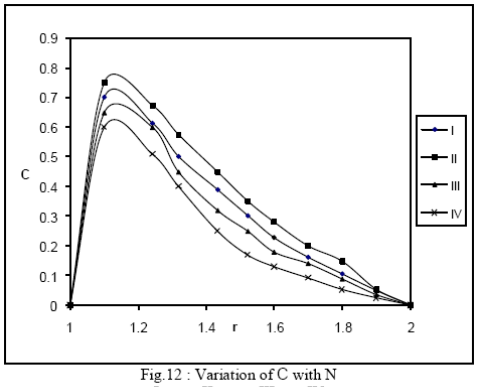

Fig.12 : Variation of C with N

	I	II	III	IV
N	1	2	-0.5	-1.5

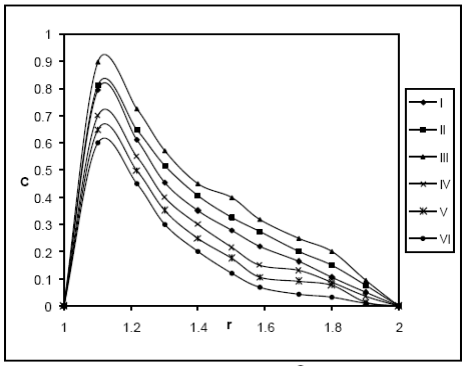

Fig.13 : Variation of C with γ

	I	II	III	IV	V	VI
γ	0.5	1.5	2.5	-0.5	-1.5	-2.5

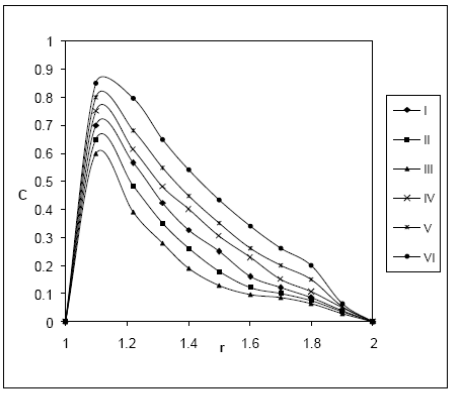

Fig.14 : Variation of C with α

	I	II	III	IV	V	VI
α	2	4	6	-2	-4	-6

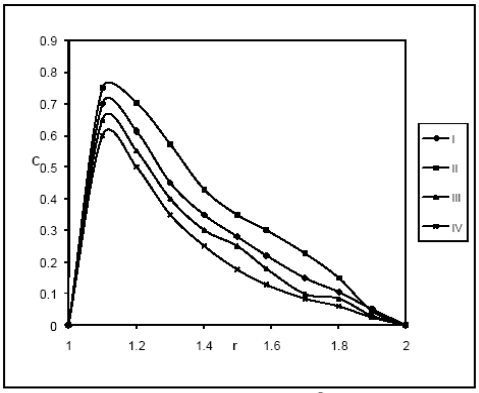

Fig.15 : Variation of C with Λ

	I	II	III	IV
Λ	0.71	1.71	3.71	7

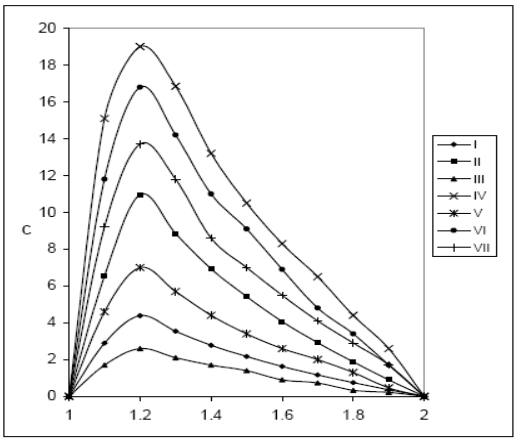

Fig.16 Variation of C with Sc&Rd

	I	II	III	IV	V	VI	VII
Sc	0.24	0.66	1.3	2.01	0.24	0.24	0.24
Rd	0.5	0.5	0.5	0.5	1.5	3.5	5

Table.2 : Shear stress, Nusselt Number and Sherwood Number

Parameter		τ(1)	τ(2)	Nu(1)	Nu(2)	Sh(1)	Sh(2)
α	**2**	0.384445	0.146087	-0.761441	15.8834	-0.029754	15.0193
	4	0.384445	-0.146085	-0.385781	16.2029	-0.029753	15.0193
	6	0.384444	-0.146083	-0.154144	16.3548	-0.029753	15.0193
	-2	0.384438	-0.146088	-1.48785	15.0969	-0.029753	15.0193
	-4	0.384435	-0.146087	-1.59238	14.9057	-0.029751	15.0193
	-6	0.384433	-0.146086	-1.57916	14.8313	-0.029753	15.0193
γ	**0.5**	1.05506	-0.952872	-0.258963	-3.97663	-0.029754	15.0193
	1.5	1.05519	-0.952958	-0.259024	-3.97711	0.08224	14.9369
	-0.5	1.05583	-0.953054	-0.259153	-3.97741	0.048159	14.9676
	-1.5	1.05607	-0.952811	-0.259004	-3.97772	-0.243983	15.2022
N	**0.5**	1.05506	-0.952872	-0.258963	-3.97663	0.252283	14.7964
	1.5	1.05512	-0.952782	-0.258947	-3.97628	0.252267	14.7964
	-0.5	1.05533	-0.95268	-0.258994	-3.98067	0.252317	14.7962
	-1.5	1.05073	-0.982207	-0.259065	-3.97027	0.252391	14.7967
Rd	**0.5**	1.05506	-0.952872	-0.258963	-3.97663	0.252283	14.7964
	1.5	1.07561	-0.97285	-0.269625	-3.99265	0.26325	14.8125
	3.5	1.09892	-0.99216	-0.27123	-4.12289	0.27425	14.8229
	5.0	1.12625	-1.01254	-0.29576	-4.23302	0.29762	14.8305
Λ	**2**	1.0533	-0.939988	-0.258074	-3.97431	0.251405	14.7965
	4	1.05283	-0.950994	-0.258428	-3.96852	0.251762	14.7968
	6	1.05837	-0.955971	-0.259781	-3.9896	0.253079	14.7957
	10	1.06152	-0.958887	-0.260567	-4.00009	0.253846	14.7952

7. CONCLUSIONS :

The coupled equations governing the flow, heat and mass transfer have been solved by using Galerkin finite method with quadratic approximation functions. The velocity, temperature and concentration have been analysed for different parametric variations. The important conclusions of the analysis are

- The velocity and temperature reduces, while the concentration enhances in the flow region with increase in N>0 when the buoyancy forces are in the same directions and for the forces acting in opposite directions, the velocity and concentration reduces while the temperature enhances The skin friction and Nusselt number reduces with N>0 and reduces with increase in N<0 on both the cylinders. The rate of mass transfer enhances on the inner cylinder and reduces on the outer cylinder with increase in N>0 when the buoyancy forces are in the same direction and for the forces acting in opposite directions ,a reversed effect is noticed in the Sherwood number.
- The velocity, temperature enhances while the concentration reduces with increase in the strength of the heat generating source and in the case of heat absorption source, the velocity reduces ,the temperature and concentration enhances in the flow region. The skin friction enhances and the Sherwood number reduces with increase in the strength of the heat generating/absorption source. The rate of heat transfer reduces on the inner cylinder and enhances on the outer cylinder with increase in $\alpha>0$ and in the case of $\alpha<0$, a reversed effect is noticed in the behaviour of Nu on the both the cylinders.
- With reference to the chemical reaction parameter γ,we find that the velocity ,temperature and concentration enhance in the flow region in the degenerating chemical reaction case while in the generating chemical reaction case, they reduces in the flow region. The skin friction and Nusselt number enhance on the cylinders with increase in $\gamma>0$ and for an increase in $\gamma<0$,the skin friction and Nusselt number reduces on the cylinders. The rate of mass transfer reduces on the outer cylinder r=2 and enhances on the inner cylinder r=1 with increase in $\gamma>0$ and with an increase in $\gamma<0$,we notice a reversed effect in the behaviour of Sh on the cylinders.

8. REFERENCES

1. Al. Nimir, M.A : Analytical solutions for transient laminar fully developed free convection in vertical annuli, Int. J. Heat and mass transfer, v. 36, pp. 2388–2395 (1993).
2. Antonio Barletta : Combined forced and free convection with viscous dissipation in a vertical duct, Int. J. Heat and mass transfer v. 42, pp. 2243–2253 (1999).
3. Chamkha, A. J., EL-Kabeir, S. M. M., and Rashad, A. M., Heat and mass transfer by non-Darcy free convection from a vertical cylinder embedded in porous media with a temperature dependent viscosity, Int. J. Numer. Methods Heat Fluid Flow, V.. 21, No. 7, pp. 847–863(2011).
4. Chen, T.S and Yuh, C.F : Combined heat and mass transfer in natural convection on inclined surface; J. Heat transfer, v. 2, pp. 233–250 (1979).

5. Madhusudha Reddy,P: Mixed convective heat and mass transfer flow through a porous medium in channel with Radiation effect. Ph. D. Thesis (2010).
6. Mallikarjuna,B,Ali J Chamkha and R ,Bhuvana Vijaya: Soret and Dufour effects on double diffusive convective flow through a non-Darcy porous medium in a cylindrical annular region in the presence of heat sources., J. Porous Media,V.17(7), pp.623-636(2014).
7. Padmavathi, A : "Finite element analysis of non-Darcian convective heattransfer through a porous medium in cylindrical & rectangular ducts with heat generating sources and radiation" "Ph. D thesis, S.K. University Anantapur, India (2009).
8. Philip, J.R: Axisymmetric free convection at small Rayleigh numbers in porous cavities. Int. J. Heat and mad transfer v. 25, pp. 1689–1699 (1982).
9. Prasad V, and Kulacki, F.A : Int. J. Heat and mass transfer, v. 27, p. 207 (1984).
10. Shaarawi, EL. M.A. I and AL. Nimir, M.A : Fully developed laminar natural convection in open ended vertical concentric annuli, Int. J. Heat and mass transfer pp. 1873–1884 (1999).
11. SivanJaneya Prasad, P : Effects of convection heat and mass transfer in unsteady hydro magnetic channels flow. Ph. D thesis S.K. University, Anantapur, India (2001).
12. Sreenivas Reddy, B : Thermo-diffusion effect on convection heat and mass transfer through a porous medium, Ph. D thesis S.K. University, Anantapur, India (2006).
13. Sreevani, M : Mixed convection heat and mass transfer though a porous medium in channels with dissipative effects, Ph. D thesis S.K. University, Anantapur, India (2003).
14. Sudarsana Reddy,P, Sreenivas,G, Sreenivasa Rao,P and Prasada Rao, D.R.V: Non-Darcy mixed convective heat and mass transfer flow of a viscous electrically conducting fluid through a porous medium in a circular annulus in the presence of temperature dependent heat sources with Soret and Dufour effects-A-finite element study.,Int.J.Comp and Appl.Math,V,.5(5),pp.595-609(2010).
15. Sudheer Kumar, Dr.M.P. Singh, Dr Rajendra Kumar : Radiation effect on natural convection in porous media; Acta Ciencia Indica v. XXXII M. No. 2, (2006).